Articles

Domain Structure of *Escherichia coli* DNA Gyrase As Revealed by Differential Scanning Calorimetry†

Michael J. Blandamer,‡ Barbara Briggs,‡ Paul M. Cullis,*,‡ Andrew P. Jackson,§,∥ Anthony Maxwell,§ and Richard J. Reece§,⊥

Departments of Chemistry and Biochemistry, Leicester University, Leicester, LE1 7RH, U.K.

Received February 17, 1994; Revised Manuscript Received April 21, 1994®

ABSTRACT: The domain structure of DNA gyrase from *Escherichia coli* has been examined using differential scanning microcalorimetry. The intact enzyme (an A_2B_2 tetramer) shows at least four transitions with apparent T_m's at 44.8, 53.3, 58.6, and 60.7 °C. Comparison with the thermal stabilities of the two separate subunits and genetically-engineered protein fragments has been used to assign these transitions to individual domains within the intact gyrase proteins. The thermal unfolding of DNA gyrase and all individual fragments are irreversible under the conditions of the calorimetric experiment. Further evidence for the assignment of transitions to particular domains has been obtained by studying the effects of tight-binding ligands such as novobiocin on the thermal stabilities of the various protein fragments.

DNA gyrase catalyses the introduction of negative supercoils into closed-circular DNA using the Gibbs energy derived from ATP hydrolysis (for a review, see Reece & Maxwell, 1991a). The enzyme from *Escherichia coli* consists of two proteins, A and B, encoded by the *gyrA* and *gyrB* genes. These genes have been sequenced and cloned such that the A and B proteins may be overproduced (Mizuuchi et al., 1984; Yamagishi et al., 1986; Swanberg & Wang, 1987; Hallett et al., 1990). The molecular masses of the A and B proteins are 97 and 90 kDa, respectively, and the active enzyme is an A_2B_2 complex (Klevan & Wang, 1980; Krueger et al., 1990).

The mechanism of DNA supercoiling by gyrase involves the following steps: (i) wrapping of a segment of DNA (ca. 120 bp) around the enzyme in a single positive superhelical turn, (ii) cleavage of the wrapped DNA in both strands with the formation of covalent bonds between the newly-formed 5′-phosphates and Tyr122 of the A subunits, (iii) passage of another segment of DNA through this double-strand break, and (iv) resealing of the broken DNA. Catalytic supercoiling is coupled energetically to the hydrolysis of ATP. In the presence of the nonhydrolyzable ATP analogue ADPNP (5′-adenylyl-β,γ-imidodiphosphate) limited supercoiling can be achieved (reviewed in Maxwell & Gellert, 1986; Reece & Maxwell, 1991a).

Gyrase is an essential enzyme in bacteria but is not present in eukaryotes. It is therefore an ideal target for antibacterial agents. Two groups of gyrase-specific drugs have been identified, the quinolones and the coumarins, both of which inhibit the DNA supercoiling reaction *in vitro* (Reece & Maxwell, 1991a). The quinolones (e.g. nalidixic acid and ciprofloxacin) are thought to act at the A subunit and interfere with the DNA breakage and reunion process. Moreover, incubation of gyrase with DNA in the presence of a quinolone drug and termination of the reaction by the addition of SDS results in the covalent attachment of the DNA to the enzyme (Gellert et al., 1977; Sugino et al., 1977). The coumarins (e.g. novobiocin and coumermycin A_1) act at the B subunit and inhibit the hydrolysis of ATP by gyrase.

There is evidence that both subunits of gyrase are organized as distinct functional domains (Figure 1). Cleavage of the gyrase A protein with trypsin yields two stable fragments of molecular masses 64 and 33 kDa (Reece & Maxwell, 1989). Bacterial clones encoding both these fragments have been engineered and the properties of the expressed proteins have been examined (Reece & Maxwell, 1991b,c). The N-terminal 64 kDa fragment contains the DNA breakage and reunion activities of the gyrase A protein and is the likely site of action of the quinolone drugs. Crystals of the 64-kDa fragment have been grown (Reece et al., 1990) but are not yet suitable for high-resolution structure determination. When complexed with the gyrase B protein, the 64-kDa fragment shows quinolone-dependent DNA cleavage activity and can inefficiently supercoil DNA. The C-terminal 33-kDa fragment has no intrinsic catalytic activity but can bind DNA and induce a positive wrap. This fragment will also enhance the weak supercoiling activity of the 64-kDa fragment complexed to the B protein. It has been suggested that these fragments may be domains of the gyrase A protein, the 64 kDa comprising the domain responsible for DNA breakage–reunion and the 33-kDa fragment comprising a domain involved in the wrapping of DNA around the A_2B_2 complex (Reece & Maxwell, 1991b,c).

The gyrase B protein has also been found to be susceptible to proteolytic cleavage, yielding two fragments of molecular masses 43 and 47 kDa (Brown et al., 1979; Gellert et al., 1979; Adachi et al., 1987; Staudenbauer & Orr, 1981; Ali et

† This work was supported by the SERC (B.B., A.P.J., and R.J.R.) and the Wellcome Trust (A.P.J.) and is a publication from the Leicester Centre for Molecular Recognition. A.M. is a Lister Institute Jenner Fellow.

* Address for correspondence: Department of Chemistry, Leicester University, University Road, Leicester LE1 7RH, UK.

‡ Department of Chemistry.

§ Department of Biochemistry.

∥ Present address: Fisons plc, Pharmaceutical Division, Loughborough, UK.

⊥ Present address: Department of Biochemistry and Molecular Biology, Harvard University, Cambridge, MA.

® Abstract published in *Advance ACS Abstracts,* June 1, 1994.

0006-2960/94/0433-7510$04.50/0

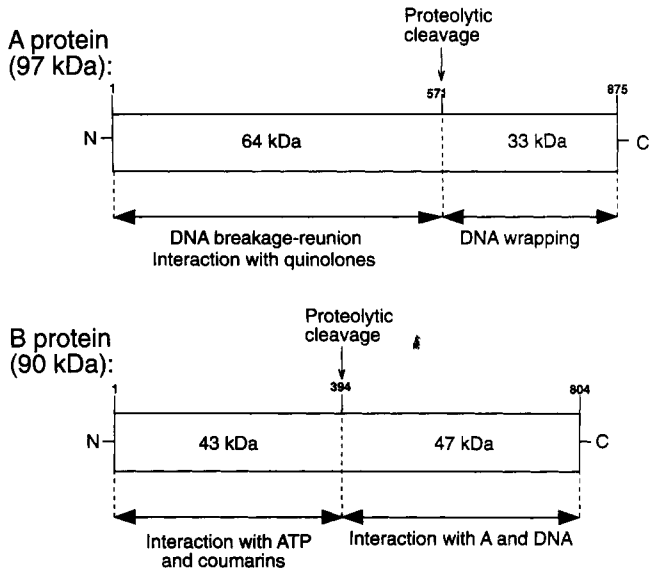

FIGURE 1: *E. coli* DNA gyrase. The enzyme consists of two proteins A and B, which form an A_2B_2 complex(M_r 374 kDa). Each protein can be subdivided into domains to which particular functions indicated above have been ascribed (Reece & Maxwell, 1991a).

al., 1993). A bacterial clone encoding the N-terminal 43-kDa fragment has been engineered and the expressed protein shown to hydrolyze ATP and bind coumarin drugs (Ali et al., 1993). This fragment has been crystallized (Jackson et al., 1991) and the structure of the protein complexed with ADPNP has been solved by X-ray crystallography to 2.5-Å resolution (Wigley et al., 1991). The C-terminal 47-kDa fragment (derived from *in vivo* proteolysis) can bind to the A protein and will support DNA relaxation but not supercoiling. Attempts to clone and overexpress this protein have been unsuccessful (Jackson & Maxwell, unpublished data). Again it is likely that these fragments represent domains of the gyrase B protein; the 43-kDa fragment comprising the ATPase moiety and the 47-kDa fragment being responsible for complexing with the A protein and DNA.

Other evidence suggestive of domain structure is provided from small-angle neutron scattering experiments (Krueger et al., 1990) which indicate that the volume of each subunit is larger than that calculated for a compact particle of the same molecular weight. In addition, electron microscopy of two-dimensional crystalline arrays of the B protein is suggestive of a protein with two asymmetric lobes (Lebeau et al., 1990). However, direct evidence is lacking. Differential scanning microcalorimetry has been extensively used to study the thermal stabilities of globular proteins (for reviews, see Privalov, 1982; Sturtevant, 1987 and references therein). We report here a study based upon differential scanning microcalorimetry (DSC) that provides direct evidence of the domain structure of DNA gyrase.

EXPERIMENTAL PROCEDURES

Protein Purification. The DNA gyrase A and B proteins were prepared as described by Hallett et al. (1990) and the A_2B_2 complex reconstituted as described by Bates and Maxwell (1989). The N- and C-terminal fragments of the gyrase A protein were prepared as described previously (Reece & Maxwell, 1991b,c) and the N-terminal fragment of the B protein prepared as described by Ali et al. (1993). Protein concentrations were determined by the method of Bradford (1976).

Calorimetry. Protein samples for calorimetry (0.5–2 mg mL^{-1}) were dialyzed into 50 mM Tris·HCl buffer (pH 7.5), 100 mM KCl, 1 mM EDTA at 4 °C with several changes of buffer. Where stated, ciprofloxacin (Bayer), novobiocin (Sigma), and ADPNP (Sigma) were added. The dependences on temperature of the differential heat capacities δC_p for DNA gyrase and for defined subunits were recorded against the reference buffer using a differential scanning microcalorimeter (Microcal MC-2, Microcal, Amherst). Subtraction of the instrument baseline from the raw data allowed analysis of the data using established procedures. Plots showing the dependence of molar heat capacity C_{pm} on temperature were constructed (Blandamer et al., 1991).

Analysis of Calorimetric Results. The dependence of molar heat capacity on temperature was analyzed using the ORIGIN software (Microcal Ltd.). The analysis proceeded through two stages.

Analysis of the data involved fitting and subtraction of a chemical baseline data derived as described above. For all systems discussed below, we found that the most satisfactory baseline (cf. ORIGIN software) that described the scan pattern over both the low and high temperature extrema of the dependence of C_{pm} on temperature was a progress curve normalized between the end points of a transition. This baseline was used to predict the baseline through the portion of the dependence of C_{pm} on temperature over the range where C_{pm} showed extrema. This constructed baseline was subtracted from the dependence of C_{pm} on temperature to yield the dependence on temperature of the molar relaxational (configurational) heat capacity, C^r_{pm}.

In the next stage of the analysis, the derived dependence of C^r_{pm} on temperature was compared with that calculated using equations based on different molecular models for the system under consideration.

Using model I, the extremum in C^r_{pm} is accounted for in terms of an equilibrium between two states, X and Y; X $\rightleftharpoons$ Y. The extremum in C^r_{pm} occurs a little above temperature T_m, where the equilibrium constant is unity. The dependence of C_{pm} on temperature is given by eq 1, where $\Delta_r H°$(vH) is the standard (van't Hoff) enthalpy of reaction.

$$C^r_{pm} = [\Delta_r H°(\text{vH})]^2 K/(1 + K)^2 RT^2 \qquad (1)$$

Then $\Delta_r H°$(vH) equals $[4\ RT_m^2 C_p(\text{max})]^{1/2}$. Further, the integral of the envelope formed by the dependence of C^r_{pm} on temperature yields the enthalpy change for the conversion of 1 mol of chemical substance X to 1 mol of chemical substance Y, $\Delta_r H°$(cal) where "cal" identifies the calorimetric enthalpy of reaction. In the textbook case, $\Delta_r H°$(vH) and $\Delta_r H°$(cal) are equal; $\Delta_r H°$(vH) describes the dependence of equilibrium constant K on temperature; cf. eq (1). In those cases where the dependences on temperature of $\Delta_r H°$(vH) and $\Delta_r H°$(cal) are small, agreement between the two derived enthalpy quantities lends support to the validity of the model in accounting for a recorded bell-shape dependence of C^r_{pm} on temperature.

In the development of this model, we assume that a complicated dependence of C^r_{pm} on temperature emerges from n independent equilibria in which no substance is common to the n equilibria. Therefore, the overall envelope showing the dependence of C^r_{pm} on temperature is characterized by n estimates of temperatures T_m and n pairs of van't Hoff and calorimetric enthalpies.

Using model II, the analysis assumes that the chemical reaction is stepwise, proceeding with increase in temperature from chemical substance X, through substance Y, to chemical substance Z. For each of the two processes, the contribution to C^r_{pm} is given by equation 2. Thus for i = 1, 2

$$C^{r}_{pm}(i) = \Delta_r H°(\mathrm{vH}i)\Delta_r H°(\mathrm{cal}i)K_i/RT^2(1 + K_i)^2 \quad (2)$$

Hence the analysis provides estimates (ORIGIN) of $T_m(1)$, $T_m(2)$, $\Delta_r H°(\mathrm{vH1})$, $\Delta_r H°(\mathrm{vH2})$, $\Delta_r H°(\mathrm{cal1})$, and $\Delta_r H°(\mathrm{cal2})$. Thus,

$$\sum_{i=1}^{i=2} \Delta_r H°(\mathrm{vH}i) \neq \sum_{i=1}^{i=2} \Delta_r H°(\mathrm{cal}i)$$

but $\sum_{i=1}^{i=2}\Delta_r H°(\mathrm{cal}i)$ yields the change in enthalpy for conversion of 1 mol of substance X to 1 mol of substance Z. The ratio $\Delta_r H°(\mathrm{cal}i)/\Delta_r H°(\mathrm{vH}i)$ yields further information concerning the nature of the domains within a protein undergoing reorganization.

In other cases the process of converting substance X to substance Z is sequential and coupled. Thus substance Y starts to produce substance Z before all of substance X has disappeared. The corresponding equation for C_{pm} includes a number of cross-terms which describe the coupling (Blandamer et al., 1984). Thus

$$C^{r}_{pm} = \Delta_r H_1°(\mathrm{cal})Q^{-1}\,dK_1/dT + \Delta_r H_1°(\mathrm{cal})K_1\,dQ^{-1}/dT + [\Delta_r H_1°(\mathrm{cal}) + \Delta_r H_2°(\mathrm{cal})]Q^{-1}\,d(K_1K_2)/dT + [\Delta_r H_1°(\mathrm{cal}) + \Delta_r H_2°(\mathrm{cal})]K_1K_2\,dQ^{-1}/dT \quad (3)$$

where

$$Q = 1 + K_1 + K_1K_2 \quad (4)$$

The ratio $\Delta_r H_i°(\mathrm{cal})/\Delta_r H_1°(\mathrm{vH})$ is not unity, measuring the extent of coupling between the two equilibria. Additional evidence is required to determine whether eq 2 or 3 is the basis of a satisfactory explanation of the dependence of C_{pm} on temperature. We have commented on these alternatives because DNA gyrase has an A_2B_2 structure.

RESULTS AND DISCUSSION

Differential scanning calorimetry offers a potentially powerful way of probing directly the domain structure of proteins. A particularly good example of this is provided by work by Privalov using scanning microcalorimetry to determine the domain organization of the terminal parts of the fibrinogen molecule (Medved' et al., 1983, 1986). We have used the same approach to determine the domain structure of *E. coli* DNA gyrase. Assignment of the specific thermal transitions to individual functional domains within the intact protein has been made by comparison with the thermal stabilities of various gyrase fragments that have been cloned and overexpressed in *E. coli*. Furthermore, the availability of tight-binding ligands whose sites of interaction are known provides another check of the assignments of the various transitions to the unfolding of particular domains. Several previous studies have demonstrated that the binding of ligands generally leads to a stabilization of the protein toward thermal denaturation. We and others have shown that this can be analyzed quantitatively in terms of the temperature dependence of two equilibria, namely the equilibrium unfolding of the protein and equilibrium binding of the substrate to the enzyme (Brandts & Lin, 1990; Blandamer & Cullis, unpublished calculations). In this present study we have used ligand binding in a purely qualitative sense to confirm our assignments of individual transitions to domains within the intact gyrase.

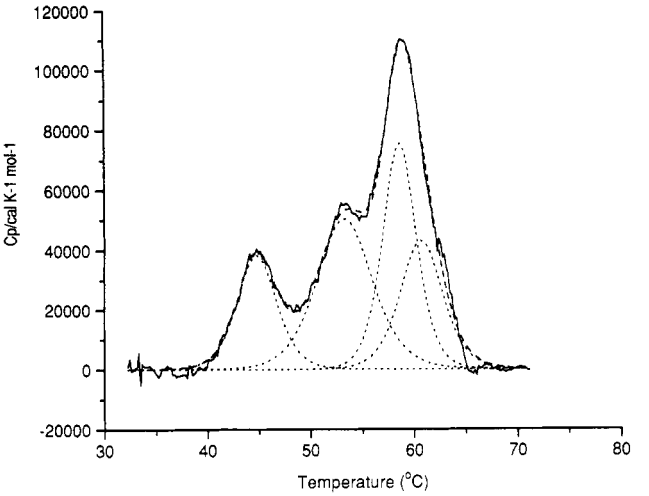

FIGURE 2: DSC scan of *E. coli* DNA gyrase (A_2B_2; protein concentration, 1.4 mg cm^{-3}; 3.7 μM in tetramer) recorded at a scan rate of ca. 60 °C/h. The data have been fitted to a tetramer using the ORIGIN software (Microcal Inc.) to four dependent transitions.

Intact DNA Gyrase. The relative heat capacity δC_p for intact DNA gyrase (A_2B_2) was recorded as a function of temperature at pH 7.5 at a scan rate of ca. 60 °C/h. The DSC trace shows three immediately identifiable maxima located at 45, 53.5, and 59 °C (Figure 2), but on the basis of deconvolution and further experiments detailed below, the high-temperature maximum at 59 °C can be shown to correspond to at least two overlapping transitions. The thermal unfolding of gyrase under these conditions is essentially irreversible in that cooling and rescanning of the sample in the calorimeter cell reveals a complete loss of all features in the DSC trace. Although the thermal denaturation appears to be irreversible, protein aggregation or precipitation does not appear to set in at temperatures immediately beyond the relevant transitions since this is invariably apparent from either a sharp fall in C_{pm} at temperatures above T_m, often accompanied by a negative spike in the thermal scan, and/or the considerable "noise" in the baseline. Despite the irreversibility of the calorimetric transitions we have followed others in the field and applied equilibrium thermodynamics to the data (Takahashi et al., 1981; Hecht et al., 1984). However, it should be noted that this is probably only valid for systems in which the irreversible step in the process is *not* taking place during the time the protein spends in the transition region (Galisteo et al., 1991). In terms of the Lumry and Ehring model (Ehring & Lumry, 1954) the equilibrium unfolding of the protein from the native (N) to the denatured state (U) is followed by an irreversible step to give a final state (F).

$$\mathrm{N} \rightleftharpoons \mathrm{U} \rightarrow \mathrm{F}$$

The nature of the irreversible step is crucial in terms of the validity of the application of equilibrium thermodynamics. For example, if the irreversible step arises from aggregation induced on rapid cooling of the calorimeter before the rescan, with the refolding from the aggregated state being extremely slow, then the DSC transition is expected to reflect a true equilibrium between the native and unfolded states. Similarly, if the irreversible step occurs at temperatures significantly higher than the denaturation temperature, then application of equilibrium thermodynamics is valid. The demonstration of a dependence of the DSC profile on the scan rate is indicative of a kinetic process, presumed to be the irreversible step. In

Table 1: Summary of the Thermodynamic Data Obtained from Analysis of the Data Shown in the Figures Using the ORIGIN Software (Microcal Inc., Amherst, MA).

protein (oligomeric form)[a]	T_m/°C	$\Delta_rH°$(cal)/kcal mol^{-1}	$\Delta_rH°$(vH)/kcal mol^{-1}
DNA gyrase (A_2B_2) (tetramer)	44.8	194	158
	53.3	358	119
	58.6	326	203
	60.7	234	163
GyrA (A_2) (dimer)	57.9	194	118
	59.7	295	141
GyrA 64-kDa fragment (dimer)	58.5	216	214
GyrA 33-kDa fragment (dimer)	42.5	92	107
GyrB 43-kDa fragment (monomer)	48.0	47	246
	49.3	55	297
GyrB 43-kDa fragment plus novobiocin (monomer)	54.2	115	244
	55.4	40	302

[a] The oligomeric form of the protein noted in brackets for each entry represents the unit that the mole refers to and was used to calculate the enthalpies.

this study for some of the DSC traces of the proteins available in large amounts we have been able to show that the DSC profiles are not dependent on scan rate. For the others, particularly that A_2B_2 complex, we cannot rule out a kinetic component. The qualitative conclusions are not affected by this.

The scan was analyzed on the basis of eq 3 using the ORIGIN software (Microcal Inc., Amherst, MA) as described above. A good fit was obtained for four sequential transitions. The deconvoluted components are shown in Figure 2 and the resulting transition temperatures and calorimetric enthalpies $\Delta_rH°$(cal) for the four features are (i) 44.8 °C and 194 kcal mol^{-1}, (ii) 53.3 °C and 358 kcal mol^{-1}, (iii) 58.6 °C and 326 kcal mol^{-1}, and (iv) 60.7 °C and 234 kcal mol^{-1}. The enthalpy change for the total denaturation of 1 mol of DNA gyrase is 1100 kcal. For each transition the corresponding van't Hoff enthalpies $\Delta_rH°(vH_i)$ were smaller that the calorimetric enthalpies. The ratios of $\Delta_rH°$(cal)/$\Delta_rH°$(vH) were all >1, indicative of the fact that the structure does not represent a single cooperative unit (see Medved' et al., 1986) but consists of at least four interacting cooperative domains. This is supported by the deconvolution analysis. All of the thermodynamic data derived from this study are summarized in the Table 1.

A Subunit. The individual subunits of DNA gyrase can be isolated and purified. To make progress on the assignment of the transitions shown in Figure 2 to the various putative domains within gyrase we studied the thermal denaturation of individual subunits. Figure 3 shows the DSC scan of the A subunit of gyrase at pH 7.5. As with the intact gyrase the denaturation under these conditions is irreversible but aggregation does not set in until much higher temperatures. The position (T_m = 58.7 °C) and appearance of the scan for the thermally induced transition for the A subunit is strikingly similar to the high-temperature transition in the scan of the intact gyrase (Figure 2). The inflexion on the high-temperature side of the absorption is even more apparent for the A subunit and a good fit of the data required a minimum of three states (two transitions). The T_m's of the two components are close and therefore we cannot distinguish between models based on two independent and two sequential processes (see above). However, on the basis of the subsequent studies on the individual domains (64 and 33 kDa), it is clear that the 33-kDa domain is considerably stabilized by interactions with the 64-kDa domain. Figure 3 therefore shows the fit for a sequential process and the ratio of the calorimetric enthalpy to the van't Hoff enthalpy is 2 and is a measure of the cooperative unfolding unit.

64-kDa N-Terminal GyrA Fragment. The domain structure and thermal stability of the 64-kDa fragment was studied

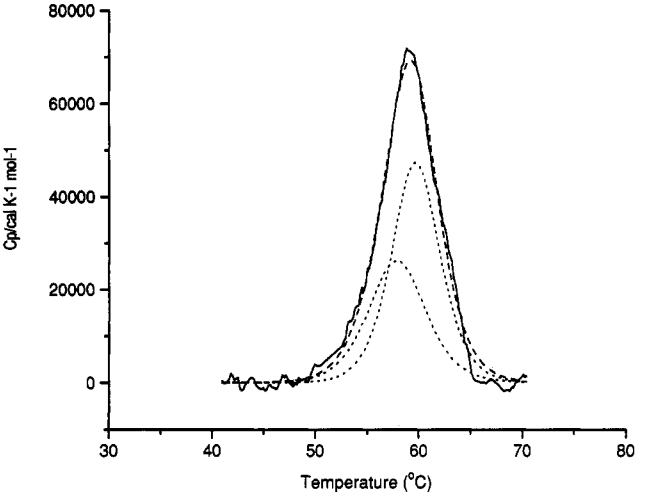

FIGURE 3: DSC scan of *E. coli* DNA gyrase A protein (protein concentration, 1.05 mg cm^{-3}; 5.5 μM in dimer) recorded at a scan rate of 60 °C/h. The data have been fitted using the ORIGIN software (Microcal Inc.) to a dimeric structure with two dependent transitions.

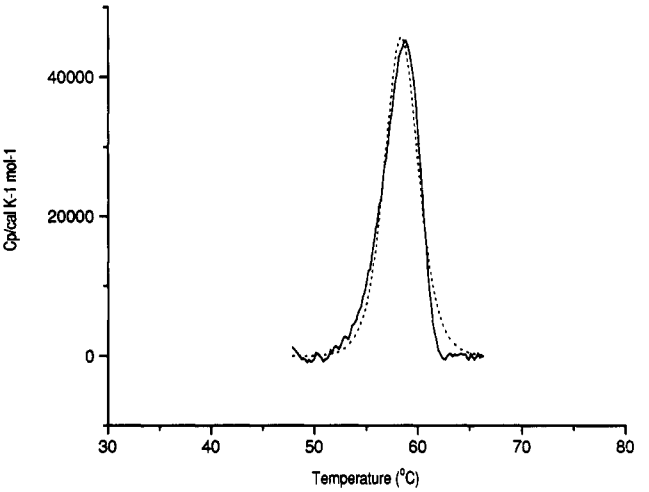

FIGURE 4: DSC scan of *E. coli* DNA gyrase 64-kDa GyrA N-terminal fragment (protein concentration, 1.15 mg cm^{-3}; 9 μM in dimer) recorded at a scan rate of 60 °C/h. The data have been fitted using the ORIGIN software (Microcal Inc.) to a dimeric structure with a single transition (X ⇌ Y).

by DSC calorimetry, and the denaturation profile is shown in Figure 4. The almost classic bell-shaped dependence of C_{pm} on temperature is satisfactorily described by eq 1, the van't Hoff and calorimetric enthalpies of reaction being in close agreement. In a qualitative analysis it seems likely from the T_m of 59 °C that this transition corresponds to the third

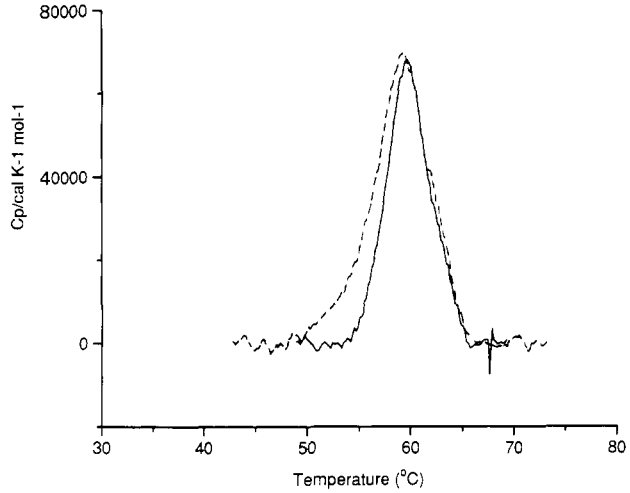

FIGURE 5: DSC scan of *E. coli* DNA gyrase A protein in the absence (broken line, from Figure 3) and presence (solid line) of ciprofloxacin (1 mM) (protein concentration, 1.05 mg cm^{-3}; 11 μM for monomeric protein).

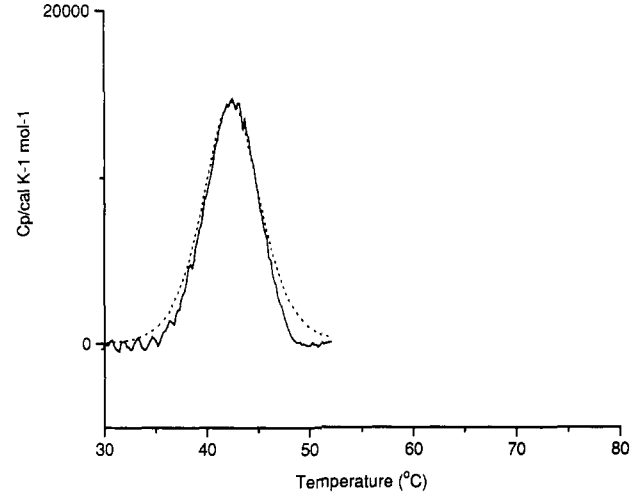

FIGURE 6: DSC scan of *E. coli* DNA gyrase 33-kDa GyrA C-terminal fragment (protein concentration, 1.55 mg cm^{-3}; 23.5 μM in dimer), recorded at a scan rate of 60 °C/h. The data have been fitted using the ORIGIN software (Microcal Inc.) to a dimer with a single domain.

transition for intact gyrase (i.e. the first transition for the A subunit). The data have been fitted assuming a dimeric structure since mechanistic considerations would suggest that this fragment must be able to dimerize. The DSC data will not fit adequately a single domain of a monomeric protein but higher order oligomers other than the dimer will fit the data (data not shown). There is evidence for the A protein being able to form tetramers which might reasonably imply that the 64-kDa GyrA is also able to form a stable tetramer (Klevan & Wang, 1980).

The quinolone drug ciprofloxacin is thought to interact with the 64-kDa domain of the A protein, as judged by point mutations to quinolone resistance which map to this region of the protein (reviewed in Maxwell, 1992). However, binding studies have failed to detect binding of a radiolabeled quinolone to GyrA or to the intact enzyme (A_2B_2); stable binding could only be detected with the gyrase–DNA complex (Willmott & Maxwell, 1993). Addition of ciprofloxacin to either the 64-kDa fragment of GyrA produced no marked shift in T_m (Figure 5), which would be in accord with the above observations. Close comparison of the DSC scans for GyrA with and without ciprofloxacin (Figure 5) shows some subtle change in the shape of the transition, with the presence of the drug appearing to reduce the assymmetry, giving rise to a slightly sharper transition. This effect is brought about by a small displacement of the lower temperature transition of GyrA which we have assigned to the 64-kDa domain. Thus the DSC may be detecting an interaction between the quinolone and the 64-kDa domain in GyrA. However, in view of the subtle nature of the changes together with failure to detect binding by other techniques discussed, any conclusions based on DSC alone should be viewed with caution.

33-kDa C-Terminal GyrA Fragment. The DSC profile for the 33-kDa protein is shown in Figure 6. As for the 64-kDa fragment above, the scan revealed a bell-shaped plot for the dependence of C°_{pm} on temperature with a T_m of 42.5 °C (Table 1). This temperature is considerably lower than either of the transitions seen in the A subunit, which provides evidence that the 33-kDa fragment, although folded, is not able to make the same contacts that it does in the A subunit. This result could imply either that the 33-kDa fragment is not able to dimerize on its own or that it gains some stabilization through interaction with the 64-kDa fragment. Both of these explanations suggest a role for the 64-kDa fragment in stabilizing

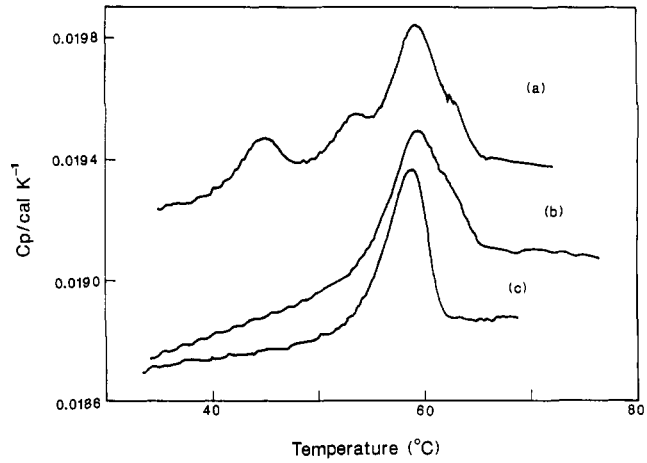

FIGURE 7: DSC scan raw data for *E. coli* DNA gyrase (a) A_2B_2 protein, (b) GyrA protein, and (c) 64-kDa GyrA fragment. The plots show the close correspondence between the thermal properties of GyrA domains in the holoenzyme, the isolated GyrA protein, and the 64-kDa fragment.

the 33-kDa fragment toward thermal unfolding. To test whether the 33-kDa fragment is indeed correctly folded but not able to make the appropriate contacts, we carried out the thermal unfolding of an equimolar mixture of the 33- and 64-kDa fragments.

The melting profile of the "reconstituted" A subunit is similar to the intact A subunit although problems of protein precipitation prevented quantitative analysis of these data (data not shown). However, qualitative analysis confirms the shift in the melting temperature of the 33-kDa fragment induced by the 64-kDa fragment even when not covalently linked. Thus the 33-kDa GyrA is correctly folded and can interact with the 64-kDa fragment, making the same contacts that exist in the intact A subunit and in the functional gyrase protein complex. It is interesting to note that the 64-kDa domain shows a similar thermal unfolding profile in the intact protein, in the GyrA subunit, and as an isolated domain (Figure 7). Thus the interaction of the 33-kDa fragment with the 64-kDa fragment leads to stabilization of the former but not vice versa.

B Subunit. Using conditions comparable to those described above, the intact B subunit was not well-behaved in the DSC experiments in that broad transitions were observed which

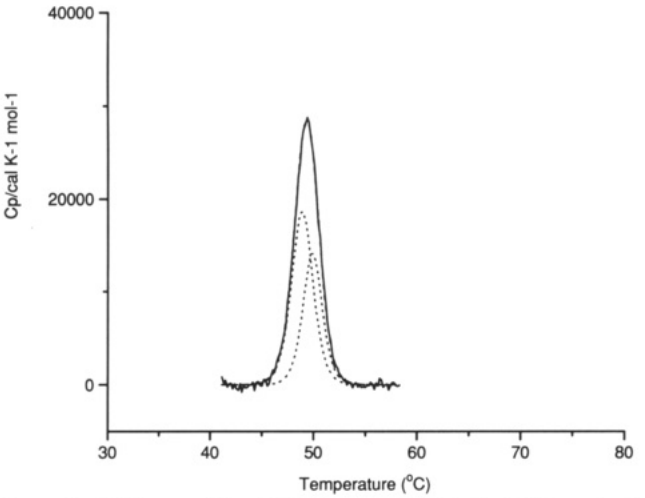

FIGURE 8: DSC scan of *E. coli* DNA gyrase 43-kDa GyrB N-terminal domain (protein concentration, 1.3 mg cm^{-3}; 30 μM for monomeric protein), recorded at a scan rate of 60 °C/h. The data have been fitted using the ORIGIN software (Microcal Inc.) to a monomer with two dependent transitions (see Figure 9).

changed with protein concentration and between batches (data not shown). Because of the dependence on protein concentration, it is likely that the problem arises from the tendency of the native B protein to form various multimeric states.

43-kDa N-Terminal GyrB Fragment. The DSC trace for the 43-kDa fragment is shown in Figure 8. Unlike the intact B protein the 43-kDa fragment is well behaved, exhibiting a smooth bell with T_m = 49.3 °C. The transition can be fitted adequately by two different models, one which assumes a single domain within a dimeric enzyme, the other assuming a two-domain monomeric protein fragment. Gel filtration and ultracentrifugation studies have shown that the 43-kDa fragment is monomeric in the absence of ATP or an ATP analogue (Ali et al., 1993). To fit the data to a monomeric protein fragment, a non-two-state model is necessary, suggesting that the 43-kDa fragment has at least two domains. Assuming the simplest model, i.e. two domains, the fit of the data is good. Fortunately, in the case of the 43-kDa GyrB fragment, the X-ray structure of the protein complexed with ADPNP is now available (Wigley et al., 1991) and shows that each monomer is comprised of two domains (Figure 9). DSC is entirely consistent with this. Furthermore, a smaller N-terminal fragment (24 kDa) of the gyrase B protein has recently been prepared (Gilbert & Maxwell, 1994) which contains the binding site for the coumarin drugs. This protein constitutes the upper part of the 43-kDa monomer shown in Figure 9 and is likely to comprise a distinct domain.

The assignment of the transitions for the 43-kDa GyrB fragment to either of the low-temperature transitions seen in the intact A_2B_2 gyrase is difficult since the T_m for the 43-kDa fragment (49 °C) falls between the two low-temperature transitions seen in the active enzyme (44.8 and 53.3 °C). On the basis of the expectation that the 43-kDa fragment is likely to be further stabilized in the functional protein, a tentative assignment of the unfolding of the 43-kDa domain to the transition at 53.3 °C in the A_2B_2 complex can be made.

Novobiocin binds to the B subunit and the 43-kDa fragment and inhibits the ATPase reaction. The estimated binding constant is thought to be $\sim 10^{-7}$–10^{-9} M (Maxwell, 1993). This allowed us to investigate the effects of novobiocin on the thermal denaturation of this domain. Tight binding of ligands to globular proteins often leads to marked stabilization of globular proteins (see Brandts & Lin, 1990). As shown in

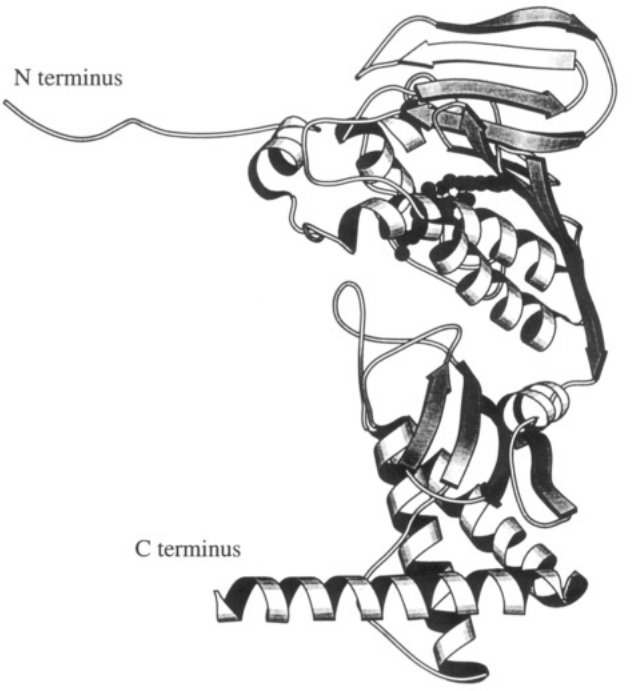

FIGURE 9: Ribbon representation of *E. coli* DNA gyrase 43 kDa GyrB fragment monomer structure based upon the X-ray crystallographic structure of the dimer 43-kDa GyrB protein in the presence of ADPNP, showing the two distinct domains (Wigley et al., 1991). The structure depicted by solid spheres associated with the top domain represents the ADPNP that is located in the crystal structure. This structure was created using the MOLSCRIPT program (Kraulis, 1991).

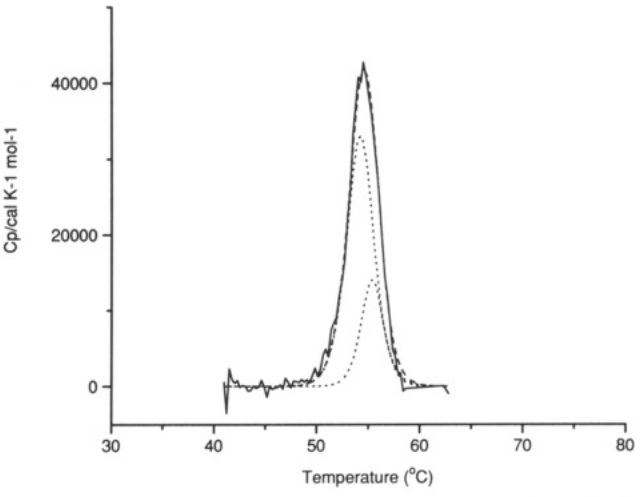

FIGURE 10: DSC scan of *E. coli* DNA gyrase 43-kDa GyrB N-terminal domain (19.7 μM monomer) in the presence of novobiocin (100 μM).

Figure 10 the inclusion of novobiocin (100 μM) leads to a major shift in T_m to higher temperature (T_m = 54.5 °C). There is an accompanying small apparent increase in enthalpy (Table 1), but we have not analyzed this fully since we have not determined the temperature dependence of the ΔH because the irreversible nature of the thermal unfolding precludes accurate determinations of the ΔC_p's.

The 43-kDa GyrB fragment crystallizes well only in the presence of ADPNP. This tight-binding ligand induces dimer formation (Ali et al., 1993) and is well-ordered in the high-resolution crystal structure. It is interesting to note that inclusion of ADPNP (1 mM) did not shift the T_m or change $\Delta_r H°$ despite the fact that this is a tight-binding inhibitor in the micromolar range. This may suggest that the binding

interaction of ADPNP shows a marked temperature dependence and that as the temperature is raised the ligand dissociates such that the observed thermal denaturation is identical to the native 43-kDa GyrB fragment on its own.

CONCLUSIONS

Using DSC we have shown that the domain structure of DNA gyrase, previously suggested from the ability to express folded proteins corresponding to various parts of the sequence, exists in the intact protein. This provides confirmation that the folded forms of the truncated proteins are closely similar to those found in the functional DNA gyrase complex. The energy-coupling process involved in the catalytic cycle requires considerable communication between the DNA binding and cleavage domains and the ATP binding and cleavage domain. In this regard, the DSC data reported here have shown that both the 33-kDa GyrA fragment, which possesses no catalytic activity but binds DNA, and the 43-kDa GyrB fragment, which is the site of ATP hydrolysis, develop important interactions in the functional protein that lead to alterations of their thermal stabilities. It is perhaps surprising that more dramatic evidence for domain interactions have not been found in view of the tight coupling between DNA cleavage and ATP hydrolysis. However, it is reasonable to assume that more profound communication between functional domains is triggered by the binding of the substrates themselves.

ACKNOWLEDGMENT

We thank Mike Sutcliffe for assistance with the molecular graphics.

REFERENCES

Adachi, T., Mizuuchi, M., Robinson, E., Apella, E., O'Dea, M., Gellert, M., & Mizuuchi, K. (1987) *Nucleic Acids Res. 15*, 771–784.

Ali, J. A., Jackson, A. P., Howells, A. J., & Maxwell, A. (1993) *Biochemistry 32*, 2717–2724.

Bates, A. D., & Maxwell, A. (1989) *EMBO J. 8*, 1861–1866.

Blandamer, M. J., Burgess, J., & Scott, J. M. W. (1984) *J. Chem. Soc., Faraday Trans. 80*, 2281–2287.

Blandamer, M. J., Briggs, B., Burgess, J., Cullis, P. M., & Eaton, G. (1991) *J. Chem. Soc., Faraday Trans. 87*, 1169–1175.

Bradford, M. M. (1976) *Anal. Biochem. 72*, 248–254.

Brandts, J. F., & Lin, L.-N. (1990) *Biochemistry 29*, 6927–6940.

Brown, P. O., Peebles, C. L., & Cozzarelli, N. R. (1979) *Proc. Natl. Acad. Sci. U.S.A. 76*, 6110–6114.

Galisteo, M. L., Mateo, P. L., & Sanchez-Ruiz, J. M. (1991) *Biochemistry 30*, 2061–2066.

Gilbert, E. J., & Maxwell, A. (1994) *Mol. Microbiol. 12*, 365–373.

Gellert, M., Mizuuchi, K., O'Dea, M. H., Itoh, T., & Tomizawa, J. (1977) *Proc. Natl. Acad. Sci. U.S.A. 74*, 4772–4776.

Gellert, M., Fisher, M., & O'Dea, M., (1979) *Proc. Natl. Acad. Sci. U.S.A. 76*, 6289–6293.

Hallett, P., Grimshaw, A. J., Wigley, D. B., & Maxwell, A. (1990) *Gene 93*, 139–142.

Hecht, M. H., Sturtevant, J. M., & Sauer, R. T. (1984) *Proc. Natl. Acad. Sci. U.S.A. 81*, 5685–5689.

Jackson, A. P., Maxwell, A., & Wigley, D. B. (1991) *J. Mol. Biol. 217*, 15–17.

Klevan, L., & Wang, J. (1980) *Biochemistry 19*, 5229–5234.

Kraulis, P. (1991) *J. Appl. Crystallogr. 24*, 946–950.

Krueger, A., Zaccai, G., Wlodawer, A., Langowski, J., O'Dea, M., Maxwell, A., & Gellert, M. (1990) *J. Mol. Biol. 211*, 211–220.

Lebeau, L., Regnier, E., Schulz, P., Wang, J., Mioskowski, C., & Oudet, P. (1990) *FEBS 267*, 38–42.

Lumry, R., & Eyring, H. (1954) *J. Phys. Chem. 58*, 110.

Maxwell, A. (1992) *J. Antimicrob. Chemother. 30*, 409–416.

Maxwell, A. (1993) *Molec. Microbiol. 9*, 681–686.

Maxwell, A. & Gellert, M. (1986) *Adv. Protein Chem. 38*, 69–107.

Medved', L. V., Gorkun, O. V., & Privalov, P. L. (1983) *FEBS Lett. 160*, 291–295.

Medved', L. V., Litvinovich, S. V., & Privalov, P. L. (1986) *FEBS Lett., 202*, 298–302.

Mizuuchi, K., Mizuuchi, M., O'Dea, M. H., & Gellert, M. (1984) *J. Biol. Chem. 259*, 9199–9201.

Privalov, P. L., (1982) *Adv. Protein Chem. 35*, 104.

Reece, R. J., & Maxwell, A. (1989) *J. Biol. Chem. 264*, 19648–19653.

Reece, R. J., & Maxwell, A. (1991a) *CRC Crit. Rev. Biochem. Mol. Biol. 26*, 335–375.

Reece, R. J., & Maxwell, A. (1991b) *J. Biol. Chem. 266*, 3546–3560.

Reece, R. J., & Maxwell, A. (1991c) *Nucleic Acids Res. 19*, 1399–1405.

Reece, R. J., Dauter, Z., Wilson, K. S., Maxwell, A., & Wigley, D. B. (1990) *J. Mol. Biol. 215*, 493–495.

Staudenbauer, W., & Orr, E. (1981) *Nucleic Acids Res. 9*, 3589–3603.

Sturtevant, J. M. (1987) *Annu. Rep. Phys. Chem. 38*, 463–488.

Sugino, A., Peebles, C. L., Kruezer, K. N., & Cozzarelli, N. R. (1977) *Proc. Natl. Acad. Sci. U.S.A. 74*, 4767–4771.

Swanberg, S., & Wang, J. (1987) *J. Mol. Biol. 197*, 792–736.

Takahashi, K., Casey, J. L., & Sturtevant, J. M. (1981) *Biochemistry 20*, 4693–4697.

Wigley, D. B., Davies, G. J., Dodson, E. J., Maxwell, A., & Dodson, G. (1991) *Nature 351*, 624–629.

Willmott, C. J. R., & Maxwell, A. (1993) *Antimicrob. Agents Chemother. 37*, 126–127.

Yamagishi, J., Yoshida, H., Yamyoshi, M., & Nakamura, S. (1986) *Mol. Gen. Genet. 204*, 367–373.